Preparation and properties of quaternary CoMoPB bulk metallic glasses

Article *in* Intermetallics · April 2016

Impact Factor: 2.13 · DOI: 10.1016/j.intermet.2015.12.008

7 authors, including:

Qiang Li

Xinjiang University

34 PUBLICATIONS **208** CITATIONS

SEE PROFILE

Li Hongxiang

University of Science and Technology Beijing

45 PUBLICATIONS **447** CITATIONS

SEE PROFILE

Jijun Zhang

Xinjiang University

6 PUBLICATIONS **10** CITATIONS

SEE PROFILE

Chuntao Chang

Ningbo Institute of Materials Technology a…

79 PUBLICATIONS **1,219** CITATIONS

SEE PROFILE

Intermetallics 71 (2016) 7–11

Contents lists available at ScienceDirect

Intermetallics

journal homepage: www.elsevier.com/locate/intermet

Preparation and properties of quaternary CoMoPB bulk metallic glasses

Luyang Bie [a], Qiang Li [a, *], Di Cao [b], Hongxiang Li [b, **], Jijun Zhang [a, c], Chuntao Chang [c], Yanfei Sun [a]

[a] School of Physics Science and Technology, Xinjiang University, Urumqi, Xinjiang 830046, PR China
[b] State Key Laboratory for Advanced Metals and Materials, University of Science and Technology, Beijing, Beijing 100083, PR China
[c] Ningbo Institute of Materials Technology & Engineering, Chinese Academy of Sciences, Ningbo, Zhejiang 315201, PR China

ARTICLE INFO

Article history:
Received 15 July 2015
Received in revised form
17 December 2015
Accepted 19 December 2015
Available online xxx

Keywords:
Metallic glasses (or amorphous metals)
Glass forming ability
Mechanical properties
Purification
Rapid solidification

ABSTRACT

A new series of $Co_{80-x}Mo_xP_{14}B_6$ (x = 7, 9, and 11 at%) bulk glassy alloys were successfully prepared by a combination method of fluxing treatment and J-quenching technique. The glass-forming ability (GFA) of the obtained Co-based alloys is sensitive to the Mo content substituted for Co, and the maximum attainable diameter for a fully amorphous state can reach 4.5 mm at $x = 9$. The compressive tests show that the obtained Co-based BMGs exhibit a compressive strength of 3.3–3.9 GPa, but nearly zero compressive plasticity. The new Co-based BMGs possess good soft magnetic properties, and their saturated magnetization values decrease from 47 emu/g (0.45 T) to 14 emu/g (0.14 T) with increasing the content of the Co substitute from 7 at% to 11 at%, which may be attributed to the anti-ferromagnetic coupling between the Mo and Co atoms. Because of their good GFA, high Co content, few constituting elements, and relatively high strength, the obtained Co-based BMGs (especially $Co_{71}Mo_9P_{14}B_6$ BMG) can be considered promising as starting alloys to develop the new Co-based BMGs for the advanced structural and functional applications.

1. Introduction

Due to many potential applications of amorphous alloys, a large number of bulk metallic glasses (BMGs) including Mg-, Ln-, Zr-, Fe-, Pd-, Ti-, Ni-, and Cu-based alloys have been developed during the last two decades [1,2]. The Co-based BMGs are most attractive for engineering applications because of their ultrahigh strength and elastic modulus values, good corrosion properties, and high oxidation resistance [3–9]. In particular, a $Co_{65-x}Ta_xB_{35}$ (x = 5–10 at%) BMG has fracture strength of 5.6–6.0 GPa and specific strength of 639–654 N m/g, which are the largest values for BMGs reported so far [4]. However, Co-based alloys generally have poor glass-forming ability (GFA), which resulted in a relatively small number of the studies about Co-based BMGs. In addition, most of the Co-based BMGs contain some amounts of the Ta element having an extremely high melting point, which makes these alloys very difficult to prepare [10]. Therefore, developing the new promising Co-based BMGs has been earnestly desired from academia to industry.

Recently, a $Fe_{80}P_{13}C_7$ BMG with a maximum diameter of 2 mm has been synthesized by combining fluxing treatment and J-quenching technique [11]. The latter was found to have unique advantages in the preparation of BMGs as compared with other conventional copper mold casting techniques [11,12]. An addition of a proper amount of the Mo element was found to effectively enhance the GFA of the Fe-based alloys [13–15]. For instance, a critical diameter for complete glass formation can be increased from 2 mm to 6 mm through the substitution of 6 at% Mo for Fe in the $Fe_{80}P_{13}C_7$ alloy [15]. Since Co is very similar to Fe in many aspects, new Co-based BMGs can be produced by adding Mo to the Co-based alloys. Thus, a new series of the $Co_{80-x}Mo_xP_{14}B_6$ (x = 7, 9, and 11 at%) alloys have been prepared, and the effects of the Mo addition on the GFA, thermal stability, and the mechanical and magnetic properties of the resulting CoMoPB BMGs were systematically investigated in the present work.

* Corresponding author.
** Corresponding author.
E-mail addresses: qli@xju.edu.cn (Q. Li), hxli@skl.ustb.edu.cn (H. Li).

http://dx.doi.org/10.1016/j.intermet.2015.12.008
0966-9795/

2. Experimental procedure

$Co_{80-x}Mo_xP_{14}B_6$ (x = 7, 9, and 11 at%) alloy ingots were prepared by torch-melting a mixture of a Co powder (99 mass % purity), Co_2P (98 mass % purity), and B pieces (99.95 mass % purity) under a high-purity argon atmosphere. All the as-prepared alloy ingots had a mass of 1–2 g. Subsequently, the ingots were fluxed at a temperature of about 1200 °C for 4–5 h under the vacuum corresponding to a residual pressure of ~50 Pa. The mixture of B_2O_3 and CaO with a mass ratio of 3.5:1 was used as a fluxing agent. After fluxing, the specimens were cooled down to an ambient temperature and then subjected to the J-quenching technique, the details of which can be found elsewhere [11,12]. As a result, $Co_{80-x}Mo_xP_{14}B_6$ alloy rods with diameters ranging from 1.0 mm to 4.5 mm and lengths of several centimeters were prepared.

The amorphous nature of the as-prepared specimens was checked by an X-ray diffractometer (XRD) using Cu K_α radiation and a scanning electron microscope (SEM) in the backscattered electron (BSE) mode. The as-prepared rod specimens were crushed into small pieces and then subjected to the XRD measurements. The thermal behavior of the as-prepared specimens was examined by differential scanning calorimetry (DSC) under an Ar atmosphere at a heating rate of 0.33 K/s. The mechanical properties of the as-prepared rods with 1 mm in diameter and 2 mm in length were measured at the ambient temperature by an uniaxial compression test conducted using an Instron testing machine at a strain rate of 2×10^{-4} s^{-1}. At least five specimens for each composition were studied by the compression test to ensure the reproducibility of the results. The magnetic properties of the as-prepared specimens were measured by a vibrating sample magnetometer (VSM) with the maximum applied field of 1.0 T at room temperature. The disc specimens with 1 mm diameter and ~0.5 mm thickness were used in the VSM measurements. A saturation magnetic field was applied parallel to the cross-section plane of the disc. The densities of the specimens were determined by the Archimedes method, and each composition was measured at least 5 times.

3. Results and discussion

Fig. 1(a) shows the XRD patterns of the as-prepared $Co_{80-x}Mo_xP_{14}B_6$ (x = 7, 9, and 11 at%) glassy alloy rods with maximum diameters (D_{max}). Only broad diffuse peaks can be observed for each pattern indicating the fully amorphous nature of the alloys. The SEM-BSE images of the as-prepared alloy rod cross-sections with the D_{max} for each composition also reveal a uniform and featureless contrast (as shown in Fig. 1(b)) further confirming the homogeneous amorphous structure of the specimens. The D_{max} values for the $Co_{80-x}Mo_xP_{14}B_6$ at x = 7, 9, and 11 are 1 mm, 4.5 mm, and 1 mm, respectively, indicating that the GFA parameters of the obtained Co-based alloys are very sensitive to the substitution content of Mo for Co.

Fig. 2 displays the DSC profiles for the as-prepared $Co_{80-x}Mo_xP_{14}B_6$ (x = 7, 9, and 11 at%) glassy alloy specimens obtained at a heating rate of 0.33 K/s. The glass transition temperature (T_g), the onset crystallization temperature (T_x), the melting temperature (T_m), and the liquidus temperature (T_l) parameters (marked by arrows in Fig. 2) are summarized in Table 1. Fig. 2(a) reveals that, except for the specimen with x = 7, the other two specimens show a clear glass transition followed by an extended supercooled liquid region and a multistage crystallization process. The T_g and T_x values of the produced Co-based BMGs shift to a higher temperature region with the increase of Mo content. The T_g and T_x of amorphous alloys are known to mainly depend on the atomic bonding strength between the constituent elements [16]. The heats of mixing for the Co–P and Co–B atomic pairs

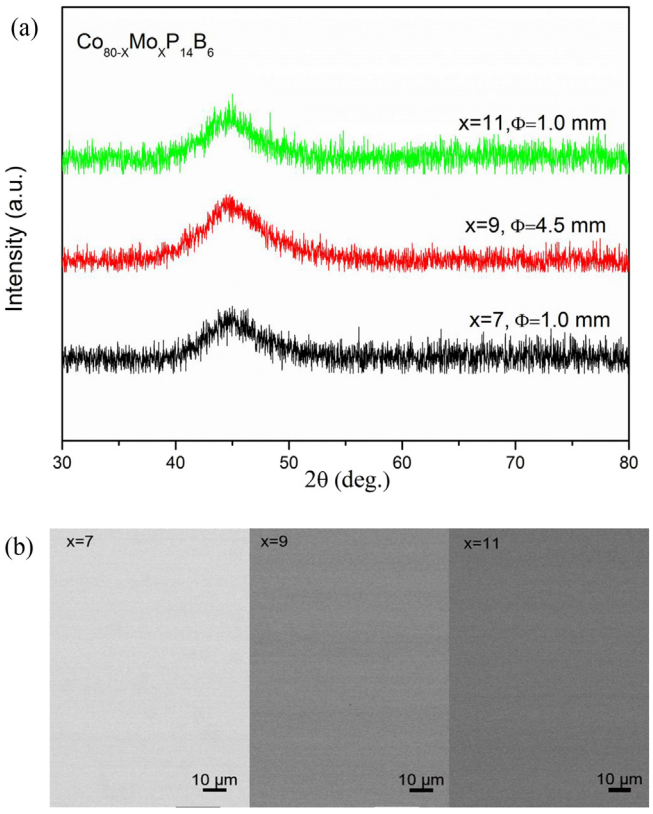

Fig. 1. XRD patterns (a) and SEM backscattered electron images obtained for the transverse section (b) of the $Co_{80-x}Mo_xP_{14}B_6$ (x = 7, 9, and 11 at%) BMGs with the critical diameters corresponding to the complete glass formation.

are −35.5 kJ/mol and −24 kJ/mol, which are much less than −53 kJ/mol and −34 kJ/mol obtained for the Mo–P and Mo–B atomic pairs, respectively [17]. Therefore, higher Mo content is expected to result in stronger bonding between the constituent elements of the Co-based BMGs leading to the higher T_g and T_x values. It should be noted that the specimen with x = 7 exhibits no obvious glass transition as indicated by the corresponding DSC thermal scan curve. The absence of T_g results in a disappearance of the supercooled liquid region for this specimen, indicating a poor ability to prevent the nucleation and growth of crystals (or bad GFA) [18], which is consistent with a low value of D_{max} (1 mm) of the specimen with x = 7.

To evaluate the GFA dependence on the Mo content in the Co-based BMGs, three common GFA parameters (the reduced glass transition temperature T_{rg} (=T_g/T_l), the supercooled liquid region ΔT_x (=$T_x - T_g$), and the parameter γ (=$T_x/(T_g + T_l)$)) were also calculated for the CoMoPB BMG specimens (see Table 1). All three GFA parameters indicate that the GFA of the $Co_{69}Mo_{11}P_{14}B_6$ alloy should be better than that of the $Co_{71}Mo_9P_{14}B_6$ alloy, which is inconsistent with our experimental D_{max} values for the produced specimens. In fact, many studies show that these GFA indicators frequently fail to evaluate the GFA of the Fe-based alloys [15,19]. Fig. 2(b) shows the details of melting patterns for the produced Co-based alloys. The alloy specimens with x = 7 and 11 exhibit two overlapping endothermic peaks, while the specimen with x = 9 seems to exhibit only a single endothermic peak or two endothermic peaks with much stronger overlapping, suggesting that the alloy with x = 9 is closer to the eutectic composition. Since the composition of an alloy with the best GFA should approach the eutectic point, the results presented here may account for the

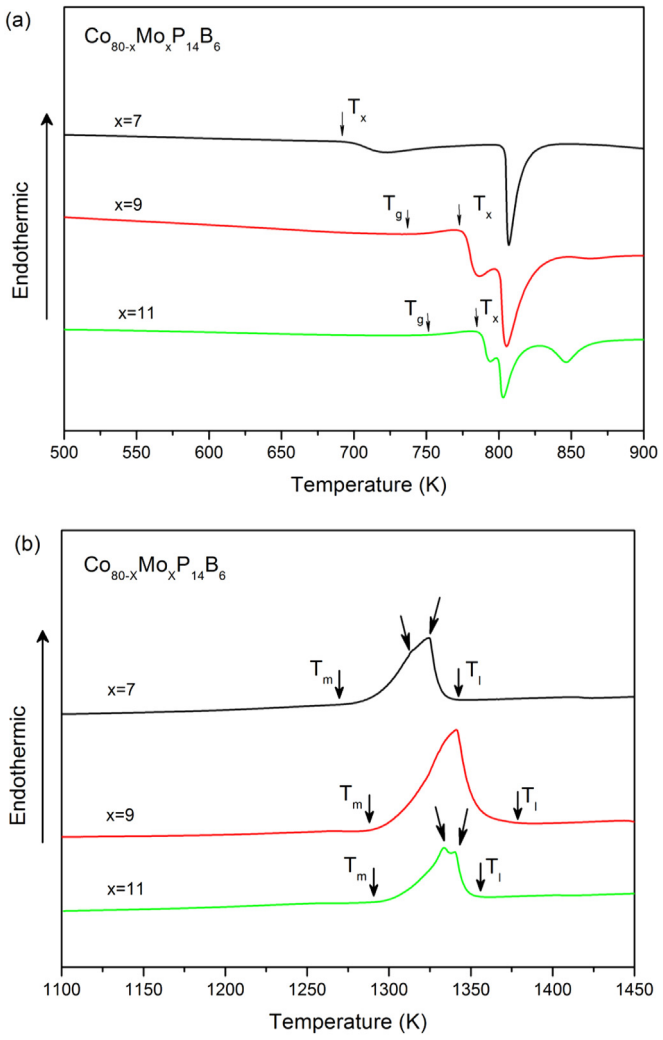

Fig. 2. DSC thermal scans from 500 K to 900 K (a) and 1100 K–1450 K (b) for the $Co_{80-x}Mo_xP_{14}B_6$ (x = 7, 9, and 11 at%) bulk glassy alloys at a heating rate of 0.33 K/s.

Table 1
A summary of the thermal properties and the GFA parameters of the as-prepared $Co_{80-x}Mo_xP_{14}B_6$ (x = 7, 9, and 11 at %) bulk glassy alloys obtained from the DSC curves at a heating rate of 0.33 K/s (D_{max}: the critical diameter for complete glass formation, T_g: glass transition temperature, T_x: onset temperature of crystallization, T_m: melting temperature, T_l: liquidus temperature, $T_{rg} = T_g/T_l$, $\Delta T_x = T_x - T_g$, $\gamma = T_x/(T_g + T_l)$).

x (at.%)	D_{max} (mm)	T_g (K)	T_x (K)	T_m (K)	T_l (K)	T_{rg}	ΔT_x (K)	γ
7	1.0	–	689	1261	1339	–	–	–
9	4.5	742	770	1290	1374	0.540	28	0.364
11	1.0	750	791	1292	1352	0.555	41	0.376

variation in the D_{max} value meaning that GFA depends on the Mo content in the obtained Co-based BMGs. In order to further understand the effect of the Mo content on the GFA of the obtained Co-based BMGs, the primary phases of the $Co_{80-x}Mo_xP_{14}B_6$ (x = 7, 9, and 11 at%) bulk glassy alloy specimens were subjected to gradual heating to a temperature that is slightly beyond the peak temperature of the first crystallization event at a heating rate of 0.33 K/s followed by a fast cooling to the room temperature in a DSC apparatus. Fig. 3 shows the corresponding XRD patterns for the heat-treated specimens. The observed crystallization peaks for the specimen with x = 7 are very weak indicating very little

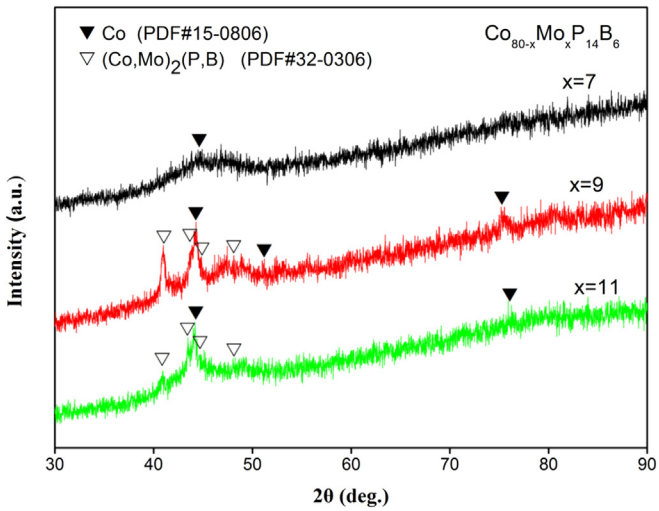

Fig. 3. XRD patterns for the $Co_{80-x}Mo_xP_{14}B_6$ (x = 7, 9, and 11 at%) bulk glassy alloys produced by gradual heating to a temperature just beyond the peak temperature of the first crystallization event at a heating rate of 0.33 K/s and then quickly cooled down to room temperature in a DSC apparatus.

crystallization. This result is also consistent with the fact that the first crystallization peak in the DSC scan of the specimen with x = 7 is very small. Both the fcc Co and $(Co,Mo)_2(P,B)$ phases appear to be parts of the primary crystalline phases for the specimens with x = 9 and 11 suggesting that the first crystallization event for these specimens corresponds to an eutectic crystallization of the fcc Co and $(Co,Mo)_2(P,B)$ phases. In addition, the crystallization phase can be quantified by the area of the corresponding crystallization peak in the XRD pattern. Fig. 3 indicates that the difference between the amounts of the fcc Co and $(Co,Mo)_2(P,B)$ phases is smaller at x = 9 than at x = 11 suggesting that the alloy with x = 9 is closer to the eutectic composition, which is also consistent with the higher GFA value for this alloy.

Fig. 4(a) shows the representative compressive stress–strain curves for the as-prepared $Co_{80-x}Mo_xP_{14}B_6$ (x = 7, 9, and 11 at%) glassy rod specimens at ambient temperature. The fracture strength σ_f and the plastic strain ε_p of the specimens determined from the compressive stress–strain curves are listed in Table 2. The fracture strength of the specimens increases from 3.30 to 3.90 GPa with the increase of the Mo substitution content from 7 to 11 at%, which is consistent with the law stating that the strength of BMGs is positively associated with T_g [20–22]. Meanwhile, the obtained Co-based BMGs appear to have almost zero compressive plasticity. Fig. 4(b) presents the SEM images of the lateral surface and fracture morphology of the specimens after compression failure. Some shear bands can be observed on the lateral surface of all the specimens. The angles between the compressive axis and the main fracture plane of the specimens with x = 7, 9, and 11 are 46°, 45.8°, and 48°, respectively, which slightly deviate from the maximum shear stress plane declined by 45° to the stress axis. Such a deviation is frequently observed for other bulk glassy alloys [23]. The fracture morphology of all the specimens exhibits poor vein-like and extensive dimple-like structures. Nanoscale periodic corrugations or nanowave structures usually appear at the fracture surfaces in brittle Fe- [24] and Mg- [25] based metallic glasses, while inflections and intersections of parallel nanowaves result in dimple-like structures [26]. The coexistence of the two morphologies indicates that the specimen experienced a rather complex stress state and an obvious crack bifurcation with serrated deformation prior to the catastrophic failure [27]. Moreover, both morphologies are

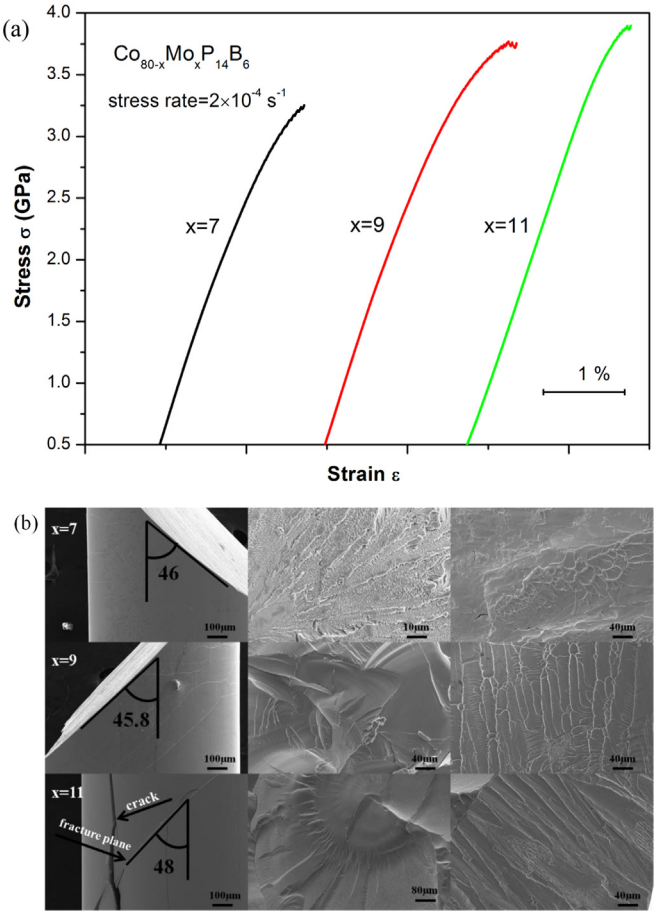

Fig. 4. (a) Representative compressive stress–strain curves for the $Co_{80-x}Mo_xP_{14}B_6$ (x = 7, 9, and 11 at%) bulk glassy alloy rods obtained at room temperature; (b) SEM images of the lateral surface and fracture morphology of the specimens after compression failure.

Table 2
A summary of the mechanical and magnetic properties of the as-prepared $Co_{80-x}Mo_xP_{14}B_6$ (x = 7, 9, and 11 at%) bulk glassy alloy rods (σ_f: compressive fracture strength, ε_p: plastic strain, J_s: saturation magnetization).

x (at.%)	Density (× 10^3 kg/m^3)	σ_f (GPa)	ε_p (%)	J_s	
				(emu/g)	(T)
7	7.82 ± 0.03	3.30	0.0	47	0.45
9	7.87 ± 0.03	3.85	0.1	25	0.24
11	7.95 ± 0.04	3.90	0.0	14	0.14

typical brittle fracture morphologies of the glass alloys and similar to other brittle Fe- and Co-based BMGs [3,6,28]. The described brittle fracture behavior and morphology further confirm the poor plasticity of the produced Co-based BMGs. It should be noted that the studied BMGs do not exhibit the expected high strength observed for the other Co-based BMGs reported earlier [4,7,9,10]. The reported compressive strengths for three representative Co-based BMGs are 5.2 GPa for $Co_{43}Fe_{20}Ta_{5.5}B_{31.5}$ [7], 5.6–6.0 GPa for $Co_{65-x}Ta_xB_{35}$ (x = 5.5–10 at%) [10], and 5.2 GPa for $Co_{61}Nb_8B_{31}$ [9], while the compressive strength of the CoMoPB BMGs is only 3.3–3.9 GPa. It is well known that the strength of BMGs follows the universal scaling rule with T_g [20–22]. The T_g values of the $Co_{43}Fe_{20}Ta_{5.5}B_{31.5}$ [7], $Co_{65-x}Ta_xB_{35}$ (x = 5.5–10 at%) [10], and $Co_{61}Nb_8B_{31}$ [9] BMGs are 910 K, 930–975 K, and ~890 K, respectively, while the T_g of the produced CoMoPB BMGs is lower than 750 K. Therefore, a relatively low compressive strength value of the obtained CoMoPB BMGs is understandable. The present work indicates that the ultrahigh strength is not a unique feature of the Co-based BMGs. The ultrahigh strength or high T_g of the previously studied Co-based BMGs may be attributed to the high content of the metalloid element B or the addition of an element with a high melting point such as Ta. The obtained results are significant for studying the mechanical properties of the Co-based BMGs and the development of new BMGs with the ultrahigh strength.

Fig. 5 illustrates the hysteresis J–H curves for the as-prepared $Co_{80-x}Mo_xP_{14}B_6$ (x = 7, 9, and 11 at%) glassy rod specimens measured by VSM at room temperature after the influence of the demagnetizing field has been corrected. The saturated magnetizations (J_s) of the specimens with x = 7, 9, and 11 obtained from Fig. 5 are 47 emu/g (0.45 T), 25 emu/g (0.24 T) and 14 emu/g (0.14 T), respectively (see Table 2). Thus, the prepared Co-based BMGs exhibit very good soft magnetic properties. Meanwhile, the J_s values of the Co-based BMGs rapidly decrease with the increase of the Mo content, which may be due to the anti-ferromagnetic coupling between the Mo and Co atoms.

4. Conclusions

In summary, the new quaternary $Co_{80-x}Mo_xP_{14}B_6$ (x = 7, 9, and 11 at%) bulk glassy rod alloys have been successfully prepared in this study by combining fluxing treatment and J-quenching technique. The critical diameters for the fully amorphous alloys at x = 7, 9, and 11 are 1 mm, 4.5 mm, and 1 mm, respectively. The compressive test results show that the compressive strength of the produced CoMoPB BMGs increases from 3.3 GPa to 3.9 GPa with increasing the substitution content of Mo for Co from 7 at% to 11 at %, and the obtained materials virtually do not possess any compressive plasticity. The magnetic tests indicate that the saturated magnetization decreases from 47 emu/g (0.45 T) to 14 emu/g (0.14 T) with increasing the substitution content of Mo for Co from 7 at% to 11 at%. The combination of a good GFA, high Co content, few constituting elements, and relatively high strength suggests that the produced CoMoPB BMGs can be potentially used as advanced structural and functional materials in the future.

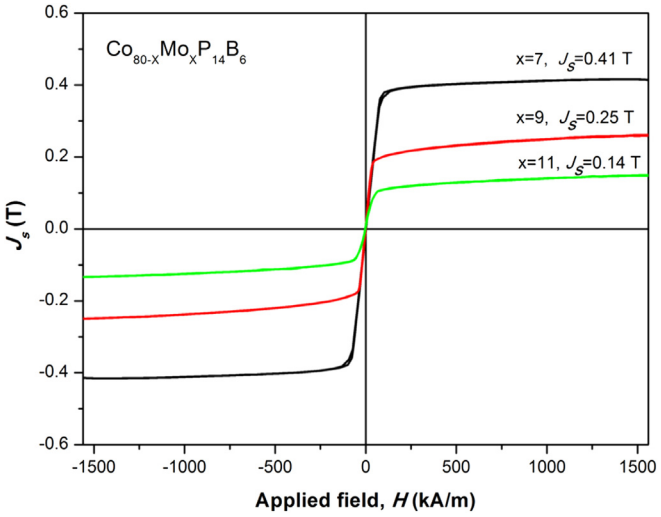

Fig. 5. Hysteresis loops for the as-prepared $Co_{80-x}Mo_xP_{14}B_6$ (x = 7, 9, and 11 at%) bulk glassy alloys obtained at room temperature.

Acknowledgments

This research was sponsored by the National Natural Science Foundation of China (Grant No. 51261028). One of the authors (Hongxiang Li) appreciates the financial support provided by the Beijing Natural Science Foundation (Grant No. 2142022) and the Program for Excellent Talents in Beijing Municipality (Grant No. 2013D0090006000004).

References

[1] W. Wang, C. Dong, C.H. Shek, Bulk Metallic Glasses, in: Materials Science and Engineering: R: Reports, 44, 2004, pp. 45–89.
[2] C. Suryanarayana, A. Inoue, Bulk Metallic Glasses, CRC Press, 2010.
[3] A. Inoue, B.L. Shen, H. Koshiba, H. Kato, A.R. Yavari, Mechanical properties of Fe-based bulk glassy alloys in Fe-B-Si-Nb and Fe-Ga-P-C-B-Si systems, J. Mater. Res. 18 (2003) 1487–1492.
[4] J.F. Wang, R. Li, N.B. Hua, T. Zhang, Co-based ternary bulk metallic glasses with ultrahigh strength and plasticity, J. Mater. Res. 26 (2011) 2072–2079.
[5] Y.Q. Dong, Q.K. Man, H.J. Sun, B.L. Shen, S.J. Pang, T. Zhang, A. Makino, A. Inoue, Glass-forming ability and soft magnetic properties of $(Co_{0.6}Fe_{0.3-}Ni_{0.1})_{67}B_{22+x}Si_{6-x}Nb_5$ bulk glassy alloys, J. Alloys Compd. 509 (2011) S206–S209.
[6] J.T. Fan, Z.F. Zhang, S.X. Mao, B.L. Shen, A. Inoue, Deformation and fracture behaviors of Co-based metallic glass and its composite with dendrites, Intermetallics 17 (2009) 445–452.
[7] A. Inoue, B.L. Shen, H. Koshiba, H. Kato, A.R. Yavari, Cobalt-based bulk glassy alloy with ultrahigh strength and soft magnetic properties, Nat. Mater. 2 (2003) 661–663.
[8] C.T. Chang, B.L. Shen, A. Inoue, Co–Fe–B–Si–Nb bulk glassy alloys with superhigh strength and extremely low magnetostriction, Appl. Phys. Lett. 88 (2006), 011901–011901-3.
[9] C.C. Dun, H.S. Liu, L. Hou, L. Xue, L.T. Dou, W.M. Yang, Y.C. Zhao, B.L. Shen, Ductile Co–Nb–B bulk metallic glass with ultrahigh strength, J. Non-Crystalline Solids 386 (2014) 121–123.
[10] J.F. Wang, R. Li, N.B. Hua, T. Zhang, Co-based ternary bulk metallic glasses with ultrahigh strength and plasticity, J. Mater. Res. 26 (2011) 2072–2079.
[11] Q. Li, J.F. Li, K.F. Yao, J.E. Gao, H.X. Li, Formation of bulk magnetic ternary $Fe_{80}P_{13}C_7$ glassy alloy, Intermetallics 26 (2012) 62–65.
[12] Q. Li, Formation of ferromagnetic bulk amorphous $Fe_{40}Ni_{40}P_{14}B_6$ alloys, Mater. Lett. 60 (2006) 3113–3117.
[13] W.H. Wang, Roles of minor additions in formation and properties of bulk metallic glasses, Prog. Mater. Sci. 52 (2007) 540–596.
[14] X. Li, C.L. Qin, H. Kato, A. Makino, A. Inoue, Mo microalloying effect on the glass-forming ability, magnetic, mechanical and corrosion properties of $(Fe_{0.76}Si_{0.096}B_{0.084}P_{0.06})_{100-x}Mo_x$ bulk glassy alloys, J. Alloys Compd. 509 (2011) 7688–7691.
[15] X.H. Yang, X.H. Ma, Q. Li, S.F. Guo, The effect of Mo on the glass forming ability, mechanical and magnetic properties of FePC ternary bulk metallic glasses, J. Alloys Compd. 554 (2013) 446–449.
[16] H.S. Chen, Glassy metals, in: Reports on Progress in Physics, 43, 1980, p. 353.
[17] A. Takeuchi, A. Inoue, Classification of bulk metallic glasses by atomic size difference, heat of mixing and period of constituent elements and its application to characterization of the main alloying element, Mater. Trans. 46 (2005) 2817–2829.
[18] A. Inoue, Stabilization of metallic supercooled liquid and bulk amorphous alloys, Acta Mater. 48 (2000) 279–306.
[19] V. Ponnambalam, S.J. Poon, G.J. Shiflet, Fe-based bulk metallic glasses with diameter thickness larger than one centimeter, J. Mater. Res. 19 (2004) 1320–2132.
[20] Y.Q. Cheng, E. Ma, Atomic-level structure and structure–property relationship in metallic glasses, Prog. Mater. Sci. 56 (2011) 379–473.
[21] P. Guan, M. Chen, T. Egami, Stress-temperature scaling for steady-state flow in metallic glasses, Phys. Rev. Lett. 104 (2010) 205701.
[22] B. Yang, C.T. Liu, T.G. Nieh, Unified equation for the strength of bulk metallic glasses, Appl. Phys. Lett. 88 (2006) 221911.
[23] Z.F. Zhang, J. Eckert, L. Schultz, Difference in compressive and tensile fracture mechanisms of $Zr_{59}Cu_{20}Al_{10}Ni_8Ti_3$ bulk metallic glass, Acta Mater. 51 (2003) 1167–1179.
[24] J.H. Yao, J.Q. Wang, Y. Li, Ductile Fe-Nb-B bulk metallic glass with ultrahigh strength, Appl. Phys. Lett. 92 (2008) 251906.
[25] G. Wang, D.Q. Zhao, H.Y. Bai, M.X. Pan, A.L. Xia, B.S. Han, X.K. Xi, Y. Wu, W.H. Wang, Nanoscale periodic morphologies on the fracture surface of brittle metallic glasses, Phys. Rev. Lett. 98 (2007) 235501.
[26] X.K. Xi, D.Q. Zhao, M.X. Pan, W.H. Wang, Y. Wu, J.J. Lewandowski, Fracture of brittle metallic glasses: brittleness or plasticity, Phys. Rev. Lett. 94 (2005) 125510.
[27] B.L. Shen, C.T. Chang, Z.F. Zhang, A. Inoue, Enhancement of glass-forming ability of FeCoNiBSiNb bulk glassy alloys with superhigh strength and good soft-magnetic properties, J. Appl. Phys. 102 (2007), 023515–023515-7.
[28] A. Inoue, B.L. Shen, C.T. Chang, Super-high strength of over 4000 MPa for Fe-based bulk glassy alloys in $[(Fe_{1-x}Co_x)_{0.75}B_{0.2}Si_{0.05}]_{96}Nb_4$ system, Acta Mater. 52 (2004) 4093–4099.